doi.org/10.1002/cbdv.202401225 Research Article CHEMISTRY & BIODIVERSITY

www.cb.wiley.com

Inhibition Effects of Some Non-Proteinogenic Amino Acid Derivatives on Carbonic Anhydrase Isoenzymes and Acetylcholinesterase: An *In Vitro* Inhibition and Molecular Modeling Studies

Zuhal Alım,*[a] Ravi Rawat,[b] Şevki Adem,[c] Volkan Eyüpoğlu,[c] and Ebru Akkemik[d]

Amino acid derivatives are molecules of interest for medicinal chemistry and drug design studies due to their important chemical properties. In this study, the inhibition effects of some non-proteinogenic amino acid derivatives (hippuric acid (**A**), *N*-(9-Fluorenylmethoxycarbonyl)-D-valine (**B**), *N*-Z-(1-Benzotriazolylcarbonyl) methylamine (**C**), (S)-N-Z-1-Benzotriazolylcarbonyl-2-phenylethylamine (**D**)) on carbonic anhydrase I (hCA-I), II (hCA-II) isoenzymes and acetylcholinesterase (AChE) activity, whose inhibitors are of vital pharmacological importance, were examined. While carbonic anhydrase (CA) inhibitors are effective molecule candidates for the treatment of many diseases from glaucoma to cancer, acetylcholinesterase inhibitors are target molecules for the treatment of Alzheimer's disease. According to the results of this study, compound **D** had a strong inhibitory effect on hCA-I (IC_{50}: 0.836 μM) and hCA-II (IC_{50}: 0.661 μM), while compound **B** (IC_{50}: 100 μM) showed a strong inhibitory effect on AChE activity. In addition, inhibition results were supported by molecular modeling studies. We hope that the obtained results will contribute to the synthesis of new and effective amino acid derivative inhibitors for CA and AChE.

Introduction

Amino acid derivatives are molecules that are the focus of interest in modern drug discovery studies[1–3] and medicinal chemistry studies because of the use of modified peptides as drugs,[4] the ease of synthesizing amino acids with various side chains, their multiple biological activities, their chiral configurations and commercial availability.[5] In the field of medicinal chemistry, amino acid derivatives are widely used as enzyme inhibitors.[5]

As a reversible process, carbonic anhydrase (CA) converts carbon dioxide (CO_2) and water into carbonic acid. The carbonic acid then dissociates into bicarbonate and hydrogen ions.[6] Numerous physiological functions are involved in this CA-catalyzed reaction, including maintaining a stable pH, breathing and gas exchange, digestion, ion transport, kidney function, and bone regeneration.[7] To date, eight different CA families (α-CAs,β-CAs,γ-CAs,δ-CAs,ζ-CAs,η-CAs,θ-CAs, and t-CAs) with different structural and functional properties have been identified.[8] There are 16 isoenzymes of α-CAs, and they are present in humans. The most researched isoenzymes among them are CA-I and CA-II, with CA-II exhibiting the greatest catalytic activity.[9] Each of these isoenzymes has different cellular localities and catalytic activities, and their behavior towards inhibitors and activators is different. Carbonic anhydrase isoenzymes have been linked to several illnesses, including cancer, glucoma, osteoporosis, neurological disorders, renal ailments, and ion transport, among others.[10,11] Therefore, carbonic anhydrase inhibitors play a large role in a wide range of biology, medicine, and drug design research.[12] These days, glaucoma patients may take one of many CA inhibitors, including Acetazolamide (AZA), Methazolamide, Dorzolamide, Brinzolamide, Diclofenamide, Ethoxazolamide, or Indisulam.[13] Apart from these, Topiramate and Zonisamide used in the treatment of epilepsy[14] and Bendroflumethiazide used in the treatment of hypertension are CA inhibitors.[15] Although many drugs that are CA inhibitors have been identified, it is an important requirement to identify new CA inhibitors that are specific to isoenzymes and have fewer side effects for the treatment of various diseases. And there are many scientific research studies on this subject. Until today, CA inhibitory properties of many compound groups such as sulfonamides, benzene sulfonamides, sulfonamides with zinc binding groups,[16] coumarins,[17] quinolines,[18] hydrazides,[19] hydrazones,[20] thiadiazole,[21] selenol[22] and catechol[23] etc. derivatives have been determined. In addition, both proteinogenic and non-proteinogenic amino acids[24] have been widely used to synthesize new CA inhibitors, considering the benefits of their chemical properties.

AChE hydrolyzes acetylcholine (ACh) to choline and acetate by cleaving the ester bond of acetylcholine. Stopping acetylcho-

[a] *Z. Alım*
Department of Chemistry, Faculty of Arts and Sciences, Kırşehir Ahi Evran University, Kırşehir, Türkiye
Tel.: +90 0544 551 81 23
E-mail: zuhal.alim@ahievran.edu.tr

[b] *R. Rawat*
Department of Pharmaceutical Sciences, School of Health Sciences and Technology, UPES University, Dehradun, India

[c] *Ş. Adem, V. Eyüpoğlu*
Department of Chemistry, Faculty of Sciences, Çankırı Karatekin University, Çankırı, Türkiye

[d] *E. Akkemik*
Faculty of Engineering, Department of Food Engineering, Siirt University, Siirt, Türkiye

line's effects in the cholinergic system is AChE's primary physiological role.[25] ACh plays a potential role in cognitive functions, particularly memory.[26] Therefore, the predominant therapeutic agents for Alzheimer's disease are AChE inhibitors, which improve cholinergic neurotransmission in the synaptic cleft by reducing the degradation of ACh.[27] For this purpose, many AChE inhibitors such as donepezil,[28] rivastigmine[29] and galantamine,[30] tacrine[31] have been developed. These drugs can provide symptomatic relief and improve cognitive impairment in patients. However, the positive effects of these AChE inhibitors are temporary and do not prevent the progression of the disease.[32,33] At the same time, the developed inhibitors have many side effects, which means that new, effective, less toxic AChE inhibitors necessitates the identification of inhibitors. Apart from many classes of compounds, studies have been conducted in which various amino acid derivatives have been evaluated as AChE inhibitors.

In this study, the inhibitory effects of some non-proteinogenic amino acid compounds (hippuric acid (**A**), *N*-(9-Fluorenylmethoxycarbonyl)-D-valine (**B**), *N*-Z-(1-Benzotriazolylcarbonyl) methylamine (**C**), (S)-N–Z-1-Benzotriazolylcarbonyl-2-phenylethylamine (**D**)) (Figure 1) on both hCA-I, hCA-II and AChE activities were investigated. Molecular modeling studies were carried out for amino acid derivatives that had an inhibitory effect.

Results and Discussion

In Vitro Inhibition Studies

Due to the function of CA isoenzymes in balancing pH and bicarbonate levels in various tissues, these isoenzymes have become valuable tools in medicinal chemistry and clinical applications.[34] CA inhibitors are of clinical importance in the treatment of various metabolic disorders, from glaucoma to cancer and even epilepsy.[35] To date, various CA inhibitors have received drug approval, but due to their side effects and nonspecificity,[36,37] there is a need to identify new, more effective and specific CA inhibitors. On the other hand, the most researched group of compounds in drug development studies for the treatment of Alzheimer's disease are AChE inhibitors. Because AChE inhibitors play a role in improving cholinergic synapses in AD disease by increasing Acetylcholine levels in the brain and thus slowing down cognitive decline.[32,33] AChE inhibitor drugs tacrine, rivastigmine, galantamine, metrifonate, and donepezil have been developed for the treatment of AD.[27] However, these drugs have very serious side effects and cannot provide a complete cure for AD disease.[27] Consequently, there are a lot of research efforts going on right now to find novel AChE inhibitors that are less toxic and more successful in fighting AD.[36] In the field of medicinal chemistry, amino acid derivatives are widely used as enzyme inhibitors. In addition, amino acid derivatives are a group of compounds that attract a lot of attention in prodrug development studies, both due to the important chemical properties of amino acids and their tendency to be transported across cell membranes. In this study, the inhibitory effects of some non-proteinogenic amino acid compounds (hippuric acid (**A**), *N*-(9-Fluorenylmethoxycarbonyl)-D-valine (**B**), *N*-Z-(1-Benzotriazolylcarbonyl) methylamine (**C**), (S)-N–Z-1-Benzotriazolylcarbonyl-2-phenylethylamine (**D**)) on both hCA-I, hCA-II and AChE activities were investigated.

The IC_{50} values, which indicate the inhibitory concentration that halves the activity, were used to assess the inhibitory effects of **A-D** compounds on hCA-I, hCA-II, and AChE. Low IC_{50} value indicates strong inhibitory effect. The molecule **A** had an inhibitory effect on both hCA-I and hCA-II isoenzymes and AChE activity. Considering the IC_{50} values for molecule **A** (IC_{50} for hCA-I: 43.04 μM, IC_{50} for hCA-II: 55.92 μM, IC_{50} for AChE: 233.3 μM) it had a stronger inhibitory effect on hCA-I and II isoenzymes than AChE. Molecule **C** did not show any inhibitory effect on either CA-I and II or AChE activity. While **B** molecule had an inhibitory effect on AChE activity (IC_{50} value of **B** for AChE: 100 μM), it did not affect the activity of hCA-I and II isoenzymes. Molecule **D** strongly inhibited the activity of hCA-I and hCA-II, but it had no inhibitory impact on AChE. For hCA-I

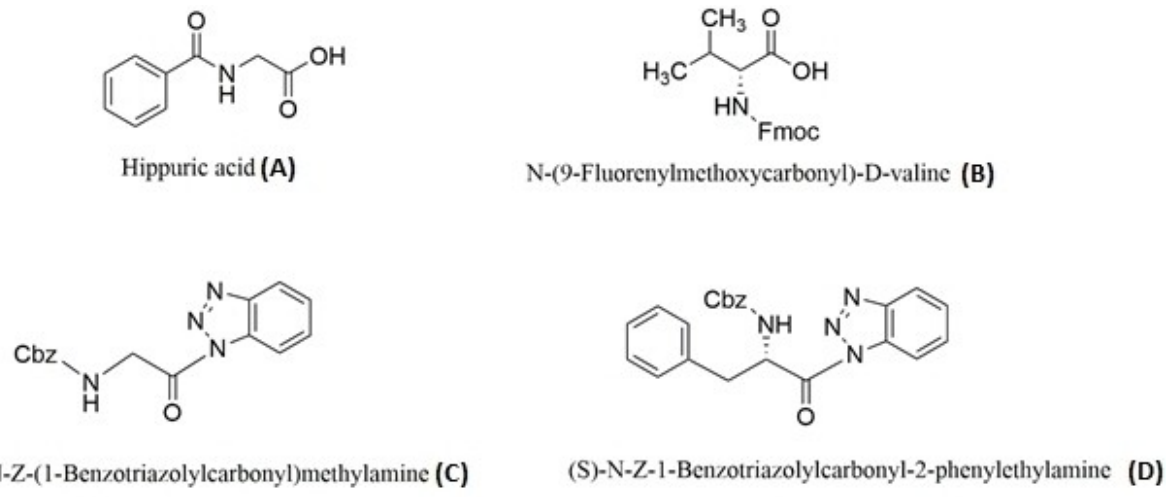

Figure 1. Non-proteinogenic amino acid compounds used in this study.

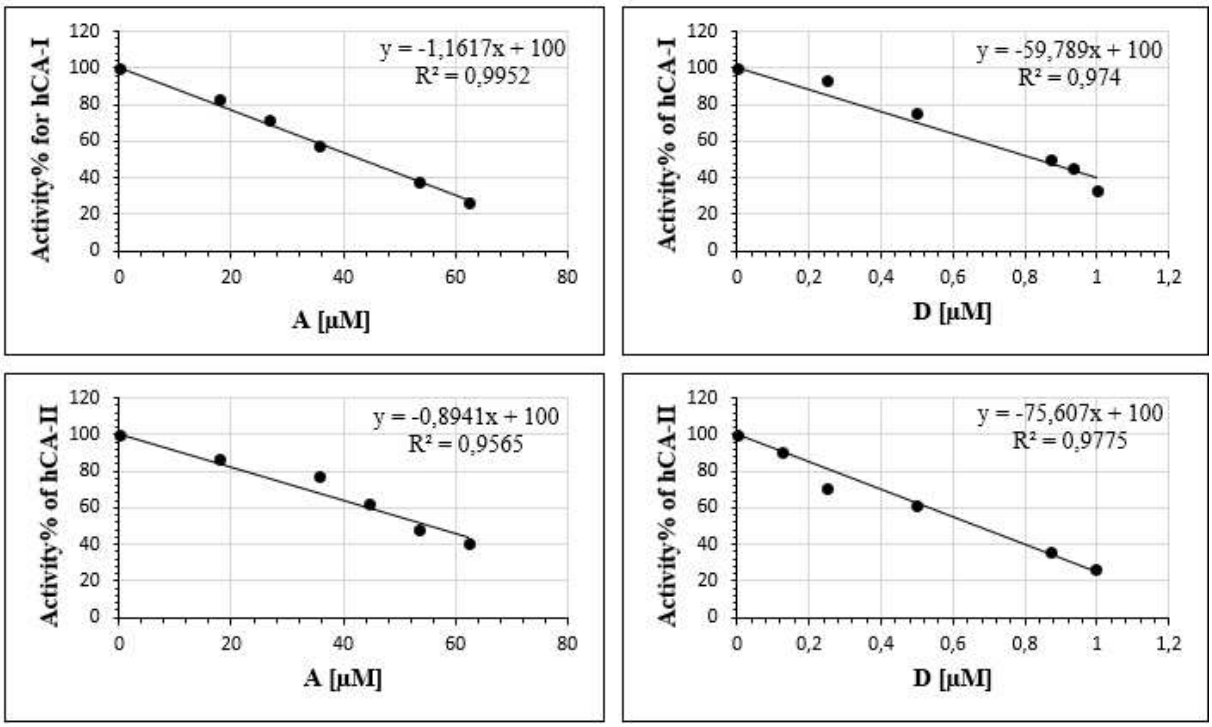

Figure 2. IC_{50} graphs of **A** and **D** for hCA-I and hCA-II.

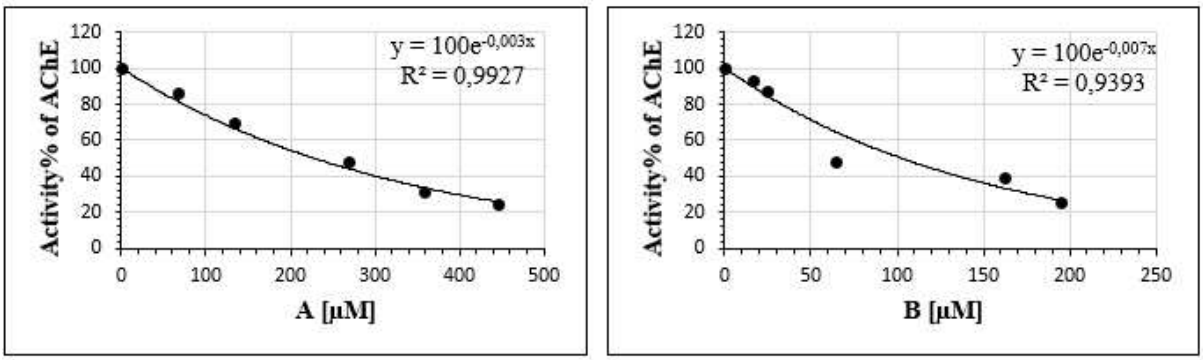

Figure 3. IC_{50} graphs of **A** and **B** for AChE.

and hCA-II, the IC_{50} values of molecule **D** were found to be 0.836 µM and 0.661 µM, respectively. Thus, for hCA-I and II isoenzymes, molecule **D** inhibited activity more effectively than molecule **A**. The results were evaluated by comparing with the reference inhibitors acetazolamide (AZA) for hCA-I, hCA-II isoenzymes and tacrine (TAC) for AChE. Figures 2 and 3 displayed IC_{50} plots, while Table 1 summarised the inhibition findings. Although the inhibitory molecules' power was lower than that of the reference inhibitors, the fact that they exhibited micromolar inhibition effects suggests they could be useful in the synthesis of novel inhibitors of amino acid derivatives. To further understand the inhibitory findings, our research also included molecular docking and molecular dynamics simulations.

Table 1. *In vitro* inhibition results.

Compounds	IC_{50} for hCA-I	IC_{50} for hCA-II	IC_{50} for AChE
A	43.04 µM	55.92 µM	233.3 µM
B	–	–	100 µM
C	–	–	–
D	0.836 µM	0.661 µM	–
AZA	0.473 µM	0.104 µM	–
TAC	–	–	0.159 µM

*AZA was used as reference inhibitor for hCA-I and hCA-II, and TAC was used as reference inhibitor for AChE.

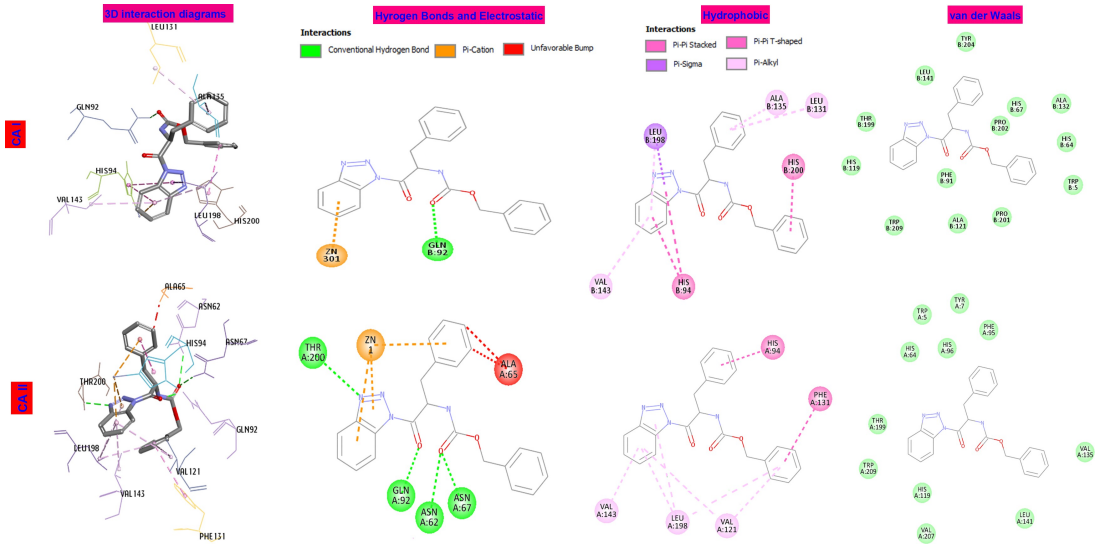

Figure 4. Interaction diagrams for hCA-I and hCA-II binding site with compound **D.**

Table 2. Important interactions of compound **D** in the hCA-I and hCA-II active cavity.

	Category	Types	Residues	Distance
hCA-II	Hydrogen Bond	Conventional Hydrogen Bond	ASN62	2.73
			ASN67	2.17
			GLN92	1.96
			THR200	2.52
	Electrostatic	Pi-Cation	ZN1	4.81
			ZN1	4.04
			ZN1	3.62
	Hydrophobic	Pi–Pi Stacked	HIS94	4.08
		Pi–Pi T-shaped	PHE131	4.71
		Pi-Alkyl	VAL121	4.87
			LEU198	5.02
			LEU198	5.05
			VAL121	5.16
			VAL143	4.98
			LEU198	5.15
hCA-I	Hydrogen Bond	Conventional Hydrogen Bond	GLN92	2.15
	Electrostatic	Pi-Cation	ZN1	3.52
	Hydrophobic	Pi-Sigma	LEU198	3.40
		Pi–Pi T-shaped	HIS94	5.50
			HIS94	5.08
			HIS200	4.35
		Pi-Alkyl	LEU131	5.06
			ALA135	3.42
			VAL143	5.11
			LEU198	4.73

Molecular Docking Studies

The binding modes predicted for the **D** into the hCA-I and hCA-II active cavity was displayed in Figure 4, and its interactions detail tabulated in Table 2. The top-ranked pose of **D** in hCA-I active region generated by Molegro Virtual Docker has −134.271 MolDock Score. It was mediating hydrogen bond interactions with the side chain residues of Gln92. The benzene rings of it formed favorable hydrophobic contacts with Leu198, Val143, His94, His200, Ala135 and Leu131 and Pi-Cation interaction with a catalytic Zn ion. Also, it interacted with Tyr199, Leu141, Tyr204, His67, Ala132, His64, Trp5, Pro201, Ala121, Phe9, Trp209 and His119 via van der Waals.

The binding energy of the compound **D** towards the hCA-II was found to be −152.271 Moldock Score. The compound showed Pi–Pi Stacked interaction with His94, Pi–Pi T-shaped interaction with Phe131, and Pi-Alkyl interactions with Val121, Leu198, Val121, Val143, and Leu198. It binds within the pocket of hCA-II by forming hydrogen bonds with Tyr200, Gln92, Asn62, and Asn67 264, and Pi-Cation interactions with the zinc ion. The docked pose of the compound shows that the 2H-benzotriazole and benzene rings of the ligand are located near the zinc ion. It takes part in the first contact by making a nucleophilic attack in the interaction with carbonic anhydrase and carbon dioxide.[38] It is thought that one of the most important factors of the strong inhibition effect of the compound on the enzyme activity may be this proximity.

CAII isoenzyme, unlike CA I, has differences in amino acid residues 62, 67 and 200. When the interaction table and 2D interaction figures are examined, it is seen that Molecule D

makes hydrogen bonds with these amino acids. It appears that this molecule interacts more with the Zn ion, which has an important role in the activity of CA enzymes, through CA-II. Unlike CA-II, isoenzyme CA-I has His200 instead of Thr200 in its active site. While molecule D makes hydrogen bond with Thr200 in its interaction with CA-II, it has a Pi–Pi T-shaped interaction with His200 in its interaction with CA-I. The results show that molecule D can interact more and stronger with CA-II through different amino acid residues. These interactions may be the reason why the molecule inhibits the CA-II isoenzyme better.

In order to obtain more information on the binding mode and interactions of the compound **B** in the active site of the AChE enzyme, molecular docking analysis was enforced. The interaction details and representations of the docking result are depicted in Table 3 and Figure 5. For it the binding affinity is found to be −145.039 MolDock Score. It interacted with the protein via both H-bond and hydrophobic contacts. The carboxyl group of the compound is localized inside the acyl and anionic binding site, making three hydrogen bonds with TYR337 and TYR341. His447 and Trp86 residues mainly contribute to the attachment of the molecule to the catalytic binding site via Pi–Pi Stacked interactions. Also, it formed Pi-Sigma interaction with TYR341 and Pi-Alkyl interaction with Tyr124, Phe338x2 and Phe297. Molecule **B** is stabilized in the AChE binding cavity mostly through van der Waals interactions with residues Trp286, Gly121, Gly122, Ser203, Glu202, Gly448, Ser125, Asp74, and THR83.

Table 3. Important interactions of compound **B** in AChE active site.

Category	Types	Residues	Distance
Hydrogen Bond	Pi-Donor Hydrogen Bond	TYR337	3.86
		TYR341	3.79
Hydrophobic	Pi-Sigma	TYR341	3.68
	Pi–Pi Stacked	TRP86	4.34
		TRP86	4.17
		TRP86	4.02
		TRP86	5.51
		HIS447	5.14
	Pi-Alkyl	TYR124	4.89
		PHE297	4.37
		PHE338	5.03
		PHE338	4.63

Molecular Dynamics Simulation

Molecular Dynamics Simulations of Human Carbonic Anhydrase I and II in Complex with LIGAND D

In order to evaluate the binding of molecule D to hCA-I (PDB ID: 6G3V) and hCA-II (PDB ID: 3PO6), we have carried out MD simulations for a period of 100 ns for two models namely, LIGAND D-hCA-I and LIGAND D-hCA-II. Several statistical metrics were used to assess their simulations, such as Root-Mean-Square-Deviation (RMSD), Root-Mean-Square-Fluctuation (RMSF), H-bond interactions, and its %occupancies over time.

RMSD Analysis

Any structural configuration that the protein goes through in the simulation may be uncovered by analysing the protein-RMSD. Figure 6 displays the multiplot for two simulations showing the relationship between protein Cα and time. Both the complexes, LIGAND **D**-hCA-I and LIGAND **D**-hCA-II has attained an equilibrium RMSD value of around 0.15 nm. The approximate value less than 0.2 nm indicates that both the complexes were stable throughout the simulation.

The stability of the ligand in relation to the protein and its binding pocket may be determined by analysing the ligand-RMSD. Figure 7 shows the multiplot of the ligand RMSD (nm) against time for two simulations. Across all simulated runs, the ligand hCA-II showed a relative improvement in deviance. The ligand hCA-I similarly ended up with an equilibrium value of 0.19 nm after displaying considerable discomfort during the simulation. When it comes to binding the hCA-I, the RMSD values shown in both situations slightly indicate that ligand hCA-II is superior than hCA-I.

RMSF Analysis

To characterise local alterations throughout the protein chain, the Protein-RMSF is helpful. In Figure 8, we can see the multiplot for protein-RMSF (nm) vs residue number index. The figure clearly shows that both ligand-protein complexes exhibited fluctuations less than 0.25 nm. Furthermore, the binding cavity residues have shown much less variation, which

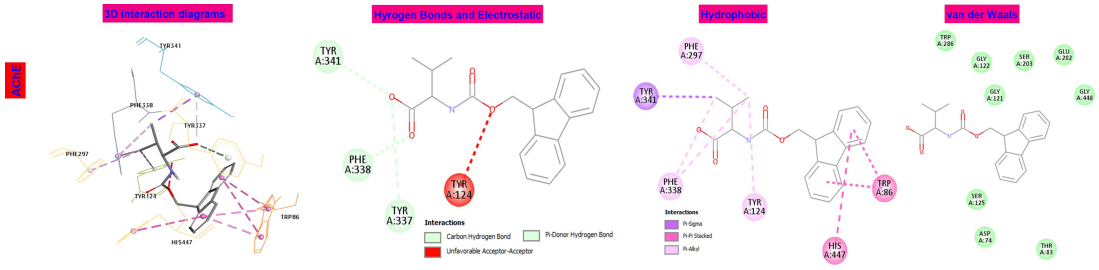

Figure 5. Interaction diagrams for AChE binding site with compound **B.**

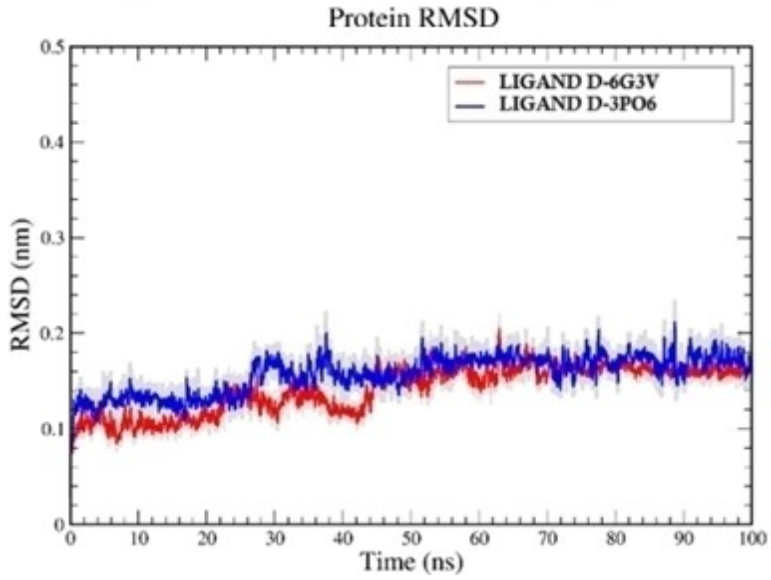

Figure 6. Graphical representation of the plots showing protein Cα RMSD (nm) versus time (100 ns) for LIGAND D-hCA-I (red in color) and LIGAND D-hCA-II (blue in color) complex.

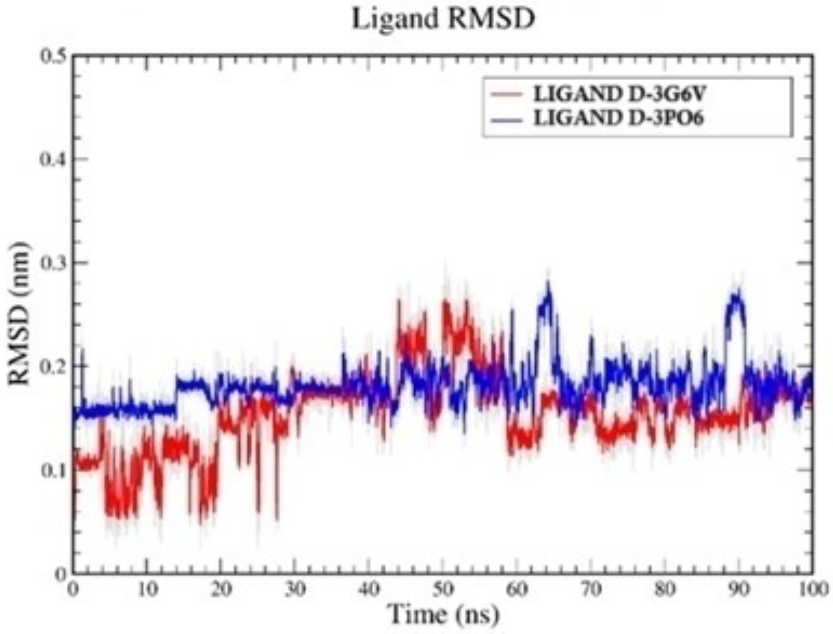

Figure 7. Graphical representation of the plots showing ligand RMSD (nm) versus time (100 ns) for LIGAND **D**-hCA-I (red in color) and LIGAND **D**-hCA-II (blue in color) complex.

indicates that the ligand is stable when it comes to binding to the protein.

H-Bond Interaction

In dynamic environments, molecular interactions, especially H-bond interactions, may be disrupted due to changes in distance and angle. In this analysis, we have examined the interactions between the ligands and proteins in both complexes. The plot for number of hydrogen vs time is being shown for LIGAND **D**-hCA-I (red in color) and LIGAND **D**-hCA-II (blue in color) complex in Figure 9. It is clear from the graphs that hCA-I and hCA-II, the ligands, have shown, on average, two stable H-bond interactions throughout the simulation.

The Figure 10, represents the histogram of %occupancies of the H-bond contacts formed by hCA-I and hCA-II, respectively. In case of hCA-I, the most stable interaction was with the residue THR199 with the occupancy of 27.52%. The other notable H-bond interactions with residues HIS200, GLN92,

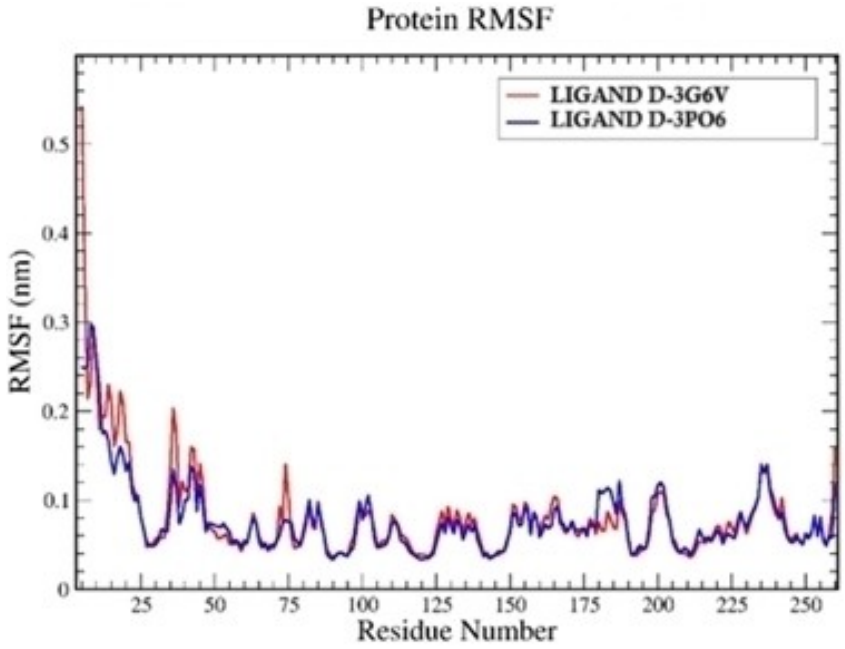

Figure 8. Graphical representation of the plots showing the protein RMSF (nm) versus residue index number of protein for LIGAND **D**-hCA-I (red in color) and LIGAND **D**-hCA-II (blue in color) complex.

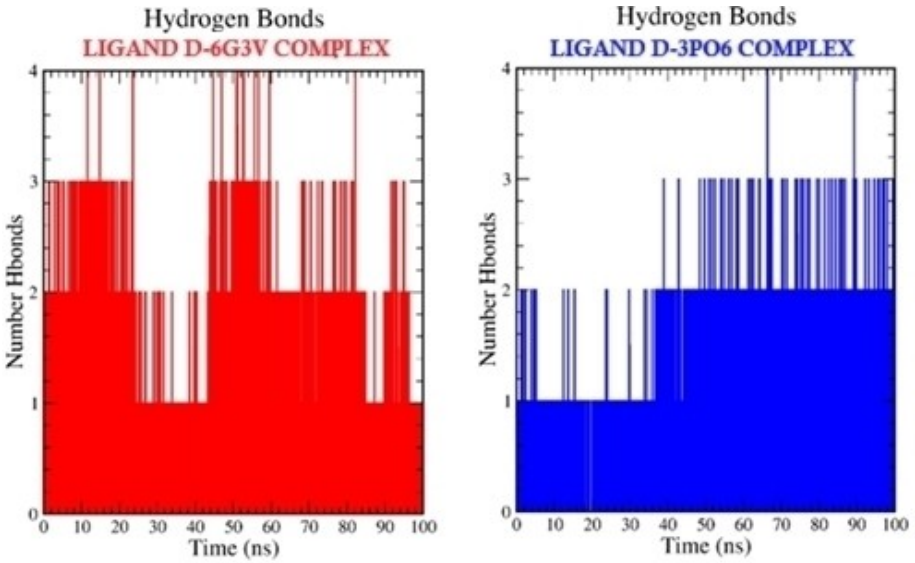

Figure 9. Pictorial representation of the number of H-bond contacts formed by ligand, hCA-I (red in color) and hCA-II (blue in color) complex.

HIS94 and HIS67 were stable for 12.02, 6.57, 6.41 and 5.81% duration of simulation. In case of hCA-II, the most stable interaction was with residue THR199, which was stable for 35.88% duration of simulation. The other weak interactions were with residues HIS200, GLN92, and HIS94 with %occupancies of 4.83, 4.28, and 3.36%, respectively. Overall, it can be concluded that both the ligands are equally efficient in binding inside the cavity of hCA-I.

Conclusions

In conclusion, it was determined that hippuric acid (**A**) and *N*-(9-Fluorenylmethoxycarbonyl)-D-valine (**B**) had an inhibitory effect on AChE activity, and hippuric acid (**A**) and (S)-N–Z-1-Benzotriazolylcarbonyl-2-phenylethylamine (**D**) showed an inhibition effect on hCA-I and HCA-II in this study. Inhibition results were supported by molecular modeling and molecular dynamics simulation studies. Molecule **D** had a MolDock Score of −134.271 for hCA-I and −152.271 for hCA-II. This result shows that molecule **D** interacts more and stronger with hCA-II

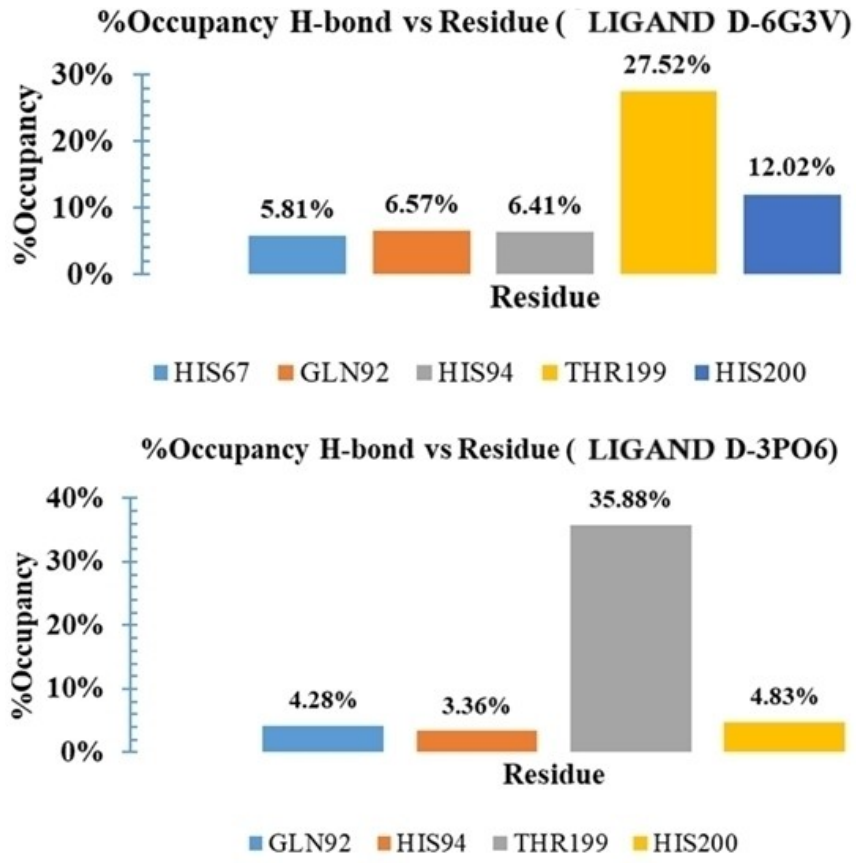

Figure 10. Histogram representation of %occupancies of the H-bond protein ligand contacts of hCA-I (Ligand D-6G3V) and hCA-II (Ligand D-3PO6) complex.

through different amino acid residues. On the other hand, since the inhibitory effect of molecule **B** on AChE activity was greater, the binding affinity (−145.039 MolDock Score) was determined by the molecular docking method and it was seen that molecule **B** interacted with AChE through both H-bonding and hydrophobic contacts. We hope that these results will guide the synthesis of new amino acid-derived carbonic anhydrase and acetylcholinesterase inhibitors.

Materials and Methods

Materials

All chemicals and amino acid compounds (hippuric acid, CAS No. 495-69-2, *N*-(9-Fluorenylmethoxycarbonyl)-D-valine, CAS No. 84624-17-9, *N*-Z-(1-Benzotriazolylcarbonyl) methylamine, CAS No. 173459-80-8, (S)-N–Z-1-Benzotriazolylcarbonyl-2-phenylethylamine, CAS No. 769922-77-2) used in the study were purchased from Sigma-Aldrich Co. (Sigma-Aldrich Chemie GmbH, Germany).

Biological Activity Studies

Inhibition Studies on hCA-I and hCA-II

As with our prior work, this study's hCA-I and hCA-II isoenzymes were isolated from human erythrocytes utilising the CNBr-activated Sepharose-4B–L-tyrosine sulfanilamide affinity chromatography technique.[39] In the isolation steps of isoenzymes, isoenzyme activities were determined by hydratase activity measurement method[40] and quantitative protein amounts were determined by Bradford protein determination method.[41] Using SDS-PAGE, we verified that the extracted isoenzymes were pure.[42] Isoenzymes that had been purified were dialyzed overnight against a 50 mM Tris-SO4 (pH 7.4) buffer. The resulting fractions were then divided into 1 mL volumes and kept at −80 °C until they were needed for biological activity tests. An approach of measuring esterase activity[43] was used when measuring the activities of hCA-I and hCA-II in inhibition studies. The substrate used in this approach was p-nitrophenyl acetate. Hydrolysis of p-nitrophenyl acetate to p-nitrophenol and acetic acid by the enzyme CA is the basis of the method's premise. An absorbance at 348 nm was measured for the p-nitrophenol that was produced throughout the process. Hence, a spectrophotometer was used to measure the absorbance at 348 nm at 25 °C in order to track the synthesis of p-nitrophenol from p-nitrophenyl acetate. The enzyme unit was calculated using the absorption coefficient ($\varepsilon = 5.4\times10^3\ M^{-1}cm^{-1}$) of p-nitrophenyl acetate at 348 nm. The inhibitory effects of **A**, **B**, **C**, and **D** compounds on hCA-I and hCA-II activities were determined by measuring at least five different concentrations of these compounds. All compounds that exhibited inhibitory effects had their percent activities measured against five distinct inhibitor concentrations using hCA-I and hCA-II. Acetazolamide, the reference inhibitor, underwent the same experiment. For both the reference inhibitor and the compounds exhibiting the inhibitory effect, graphs of Activity% against inhibitor concentration were created. The control activity was taken as 100 %. The IC_{50} values, which show

the concentration of inhibitor that reduces enzyme activity by half, were calculated from these graphs.

Inhibiton Studies on AChE

Sigma-Aldrich supplied the *Electrophorus electricus* (electrical eel) AChE (CAS no. 9000–81-1) enzyme used in the research. Using the spectrophotometric approach provided, the inhibitory impact of chemicals **A**, **B**, **C**, and **D** on AChE activity was investigated.[44] The Ellman method is a sensitive and reliable method for measuring acetylcholine esterase enzyme activity. The substrate used in this reaction is acetylthiocholine iodide. Acetylthiocholine may be transformed into thiocholine and acetic acid by the action of AChE. Mixing the reaction media with 5,5′-dithiobis (2-nitrobenzoic acid) (DTNB) causes the thiocholine that was produced during the reaction to react. The products of this chemical reaction are choline and 5-thio-2-nitrobenzoic acid. The spectrophotometric measurement of 5-thio-2-nitrobenzoic acid, a yellow chemical, may be taken at 412 nm. The inhibitory effects of **A-D** on AChE activity were determined by measuring AChE activity at least five concentrations for **A-D** compounds. For substances that exhibited inhibitory actions, we computed the percent activities of AChE against five distinct doses of inhibitors. Tacrine, the reference inhibitor, underwent the same experiment. For both the reference inhibitor and the compounds exhibiting the inhibitory effect, graphs of Activity% against inhibitor concentration were created. The control activity was taken as 100%. The IC_{50} values, which show the concentration of inhibitor that reduces enzyme activity by half, were calculated from these graphs.

Molecular Docking Studies

The 3D crystal structures of AChE (PDB code 4EY7), hCA-I (PDB code 6G3V), and hCA-II (PDB code 3PO6) were received from the Protein Data Bank website.[45–47] Compounds' three-dimensional molecular structures were obtained from the PubChem database. The MolDock Score function was used to do molecular docking calculations in Molegro Virtual Docker.[48] For docking studies, a region on the crystal structures where the inhibitor is placed in the center was selected. Co-crystal ligand was docked again with different parameters. Among the protocols that gave root mean-squared deviation (RMSD) values below 20 Å, those closest to zero were selected for docking studies of the molecules. The best-docked pose was taken into account for each compound in docking studies. The Discovery Studio 2021 Client was used to visualize interaction at the molecular level of the docking experiments.

Molecular Dynamic Simulation

In order to simulate molecular dynamics (MD), GROMACS 2022.2 was used. These procedures were employed.

Preparation of Enzyme

Pymol was used to export the three-dimensional (3D) models of the hCA-I enzyme complex with CA-I and CA-II molecules to the pdb format (PDB ID: 6G3V). In order to assess the complexes' dynamic behaviour, the GROMACS package programme (version 2022.2) was used for molecular dynamic (MD) simulation.[49–52] The protein topology was created using the SwissParam service, and the ligand topology was built using pdb2gmx with the CHARMM27 force field47.[53]

Setting up System for Simulation

The complexes were introduced into the system after the application of the force field. Using periodic boundary constraints, they were solvated in a cubic box that was more than 1 nm from the protein's edge using the SPC water model.[54] We used the steepest descent approach to minimise energy for 50,000 steps after injecting Na^+ ions neutralised the solution. The system was then equilibrated by simulating 100 ps of NVT at 300 K and 100 ps of NPT. Proteins, ligands, water molecules, and ions were all individually coupled in the constant-temperature, constant-pressure (NPT) ensemble using the leapfrog method.[55] The system was maintained in a stable environment with the Berendsen temperature coupling constant set to 1 and the pressure coupling constant to 2, respectively. The temperature was 300 K and the pressure was 1 bar.[56] Lastly, at 300 K, an isothermal and isobaric condition ensemble was used to conduct MD simulations for 100 ns. The bond lengths were constrained using the LINCS algorithm,[57] and the pressure coupling with time-constant was set at 1 ps to keep the pressure constant at 1 bar. At 1.2 nm, the Van der Waals and Coulomb interactions were terminated, and to reduce the resulting error, the PME algorithm[58] that is incorporated into GROMACS was used.

Visualization and Analysis of Simulation

The trajectory files are visualized through VMD (Visual Molecular Dynamics) 1.9.2.[59] and analyzed by indigenously developed tool HeroMDAnalysis[60,61] and Xmgrace 5.1.25.[62]

Author Contributions

Zuhal Alım carried out inhibition studies. Ravi Rawat, Şevki Adem, Volkan Eyüpoğlu did the molecular docking and molecular dynamic simulation studies. Analysis of the results and writing of the article were carried out by Zuhal Alım, Rawi Rawat, Şevki Adem, Volkan Eyüpoğlu and Ebru Akkemik.

Acknowledgements

The authors thank to Ahi Evran University Research Fund Accounting for their support to carry out this work (Project number: FEF. A4. 22. 004).

Conflict of Interests

The authors have no conflicts of interest to disclose.

Data Availability Statement

Data will be made available on request.

Keywords: Amino acids · Carbonic anhydrase · Acetylcholinesterase · Enzyme inhibition · Molecular docking

[1] K. H. Park, M. J. Kurth, *Tetrahedron* **2002**, *58*, 8629–8659. https://doi.org/10.1016/S0021-9673(00)80174-0.
[2] S. S. Katiyar, V. Kushwah, C. P. Dora, R. Y. Patil, S. Jain, *AAPS PharmSciTech* **2019**, *20*, 186. https://doi.org/10.1208/s12249-019-1396-x.
[3] B. L. De Sausa, J. P. Leite, T. A. De Oliveira Mendes, E. V. V. Varejao, A. C. S. Chaves, J. G. Silva, A. P. Agrizzi, P. G. Ferreira, E. Pilau, E. Silva, M. H. Dos Santos, *J. Braz. Chem. Soc.* **2021**, *32*, 652–664. https://doi.org/10.21577/0103-5053.20200219.
[4] K. Fosgerau, T. Hoffmann, *Drug Discovery Today* **2015**, *20*, 122–128. https://doi.org/10.1016/j.drudis.2014.10.003.
[5] M. A. T. Blaskovich, *J. Med. Chem.* **2016**, *59*, 10807–10836. https://doi.org/10.1021/acs.jmedchem.6b00319.
[6] M. Gümüş, Ş. N. Babacan, Y. Demir, Y. Sert, İ. Koca, İ. Gülçin, et al. *Archiv De Pharmazie* **2022**, 355, e2100242. https://doi.org/10.1002/ardp.202100242.
[7] R. Occhipinti, W. F. Boron, *Int. J. Mol. Sci.* **2019**, *20*, 3841. https://doi.org/10.3390/ijms20153841.
[8] F. S. Tokalı, Z. Alım, Ü. Yırtıcı, *ChemistrySelect* **2023**, *8*, e202204191. https://doi.org/10.1002/slct.202204191.
[9] I. Hassan, B. Shajee, A. Waheed, F. Ahmad, W. S. Sly, *Bioorg. Med. Chem.* **2013**, *21*, 1570–1582. https://doi.org/10.1016/j.bmc.2012.04.044.
[10] C. T. Supuran, *Biochem. J.* **2016**, *473*, 2023–2032.https://doi.org/10.1042/BCJ20160115.
[11] M. Y. Mboge, B. P. Mahon, R. McKenna, S. C. Frost, *Metabolites* **2018**, *8*, 19. https://doi.org/10.3390/metabo8010019.
[12] R. McKenna, C. T. Supuran, *Subcell. Biochem.* **2014**, *75*, 291–323.
[13] S. Kumar, S. Rulhania, S. Jaswal, V. Monga, *Eur. J. Med. Chem.* **2021**, *209*, 112923, https://doi.org/10.1016/j.ejmech.2020.112923.
[14] L. Ciccone, C. Cerri, S. Nencetti, E. Orlandini, *Molecules* **2021**, *26*, 6380. https://doi.org/10.3390/molecules26216380.
[15] P. Pickkers, R. S. Garcha, M. Schachter, P. Smits, A. D. Hughes, *Hypertension* **1999**, *33*, 1043–1048. https://doi.org/10.1161/01.HYP.33.4.1043.
[16] C. T. Supuran, A. Scozzafava, A. Casini, *Med. Res. Rev.* **2003**, *23*, 146–189. https://doi.org/10.1002/med.10025.
[17] A. Maresca, C. Temperini, H. Vu, N. B. Pham, S. A. Poulsen, A. Scozzafava, R. J. Quinn, C. T. Supuran, *J. Am. Chem. Soc.* **2009**, *131*, 3057–3062. https://doi.org/10.1021/ja809683v.
[18] P. S. Thacker, P. Shaikh, A. Angeli, M. Arifuddin, C. T. Supuran, *J. Enzyme Inhib. Med. Chem.* **2019**, *34*, 1172–1177. https://doi.org/10.1080/14756366.2019.1626376.
[19] H. Shirinzadeh, E. Dilek, *J. Mol. Struct.* **2020**, *1220*, 128657. https://doi.org/10.1016/j.molstruc.2020.128657.
[20] V. Sharma, R. Kumar, S. Bua, C. T. Supuran, P. K. Sharma, *Bioorg. Chem.* **2019**, *85*, 198–208. https://doi.org/10.1016/j.bioorg.2019.01.002.
[21] M. Abas, A. Bahadur, Z. Ashraf, S. Iqbal, M. S. R. Rajoka, S. G. Rashid, E. Jabeen, Z. Iqbal, Q. Abbas, A. Bais, M. Hassan, G. Liu, K. Feng, S. H. Lee, M. Nawaz, M. A. Qayyum, *J. Mol. Struct.* **2021**, *1246*, 131145. https://doi.org/10.1016/j.molstruc.2021.131145.
[22] A. Angeli, D. Tanini, A. Nocentini, A. Capperucci, M. Ferranoni, P. Gratteri, C. T. Supuran, *Chem. Commun.* **2019**, *55*, 648–651. https://doi.org/10.1039/c8cc08562e.
[23] K. D'Ambrosio, S. Carradori, S. Cesa, A. Angeli, S. M. Monti, C. T. Supuran, G. De Simone, *Chem. Commun.* **2020**, *56*, 13033–13036. https://doi.org/10.1039/D0CC05172A.
[24] N. Chiaramonte, M. N. Romanelli, E. Teodori, C. T. Supuran, *Metabolites* **2018**, *8*(2), 36. https://doi.org/10.3390/metabo8020036.
[25] V. Tougu, *Current Med. Chem.: Cent. Nerv. Syst. Agents* **2001**, *1*, 155–170. https://doi.org/10.2174/1568015013358536.
[26] A. Blokland, *Brain Res. Rev.* **1995**, *21*, 285–300. https://doi.org/10.1016/0165-0173(95)00016-x.
[27] A. Nordberg, A. L. Svensson, *Drug Saf.* **1998**, *19*, 465–480. https://doi.org/10.2165/00002018-199819060-00004.
[28] S. Akasofu, M. Kimura, T. Kosasa, K. Sawada, H. Ogura, *Chem.-Biol. Interact.* **2008**, *175*, 222–226. https://doi.org/10.1016/j.cbi.2008.04.045.
[29] B. R. Williams, L. A. Nazarians, M. A. Giii, Clinical *Therapeutique* **2003**, *25*, 1634–1653. https://doi.org/10.1016/s0149-2918(03)80160-1.
[30] M. Gauding, U. Richarz, J. Han, B. V. Baelen, B. Schauble, *Curr. Alzheimer Res.* **2011**, *8*, 771–780. https://doi.org/10.2174/156720511797633205.
[31] J. S. Kelly, *Trends Pharmacol. Sci.* **1999**, *20*, 127–129. https://doi.org/10.1016/s0165-6147(99)01344-9.
[32] H. Ullah, F. Rahim, H. Zada, S. Hayat, F. Khan, M. S. Khan, *Chem. Data Collect.* **2023**, *46*, 101048. https://doi.org/10.1016/j.cdc.2023.101048.
[33] H. Ullah, M. Jabeen, F. Rahim, A. Hussain, F. Khan, M. Perviaz, M. Sajid, I. Uddin, M. U. Khan, M. Nabi, *Chem. Data Collect.* **2023**, *44*, 100988. https://doi.org/10.1016/j.cdc.2022.100988.
[34] M. Y. Mboge, B. P. Mahon, R. McKenna, S. C. Frost, *Metabolites* **2018**, *8*, 19, https://doi.org/10.3390/metabo8010019.
[35] C. B. Mishra, M. Tiwari, C. T. Supuran, *Med. Res. Rev.* **2020**, *40*, 2485–2565. https://doi.org/10.1002/med.21713.
[36] Z. Alım, Z. Köksal, M. Karaman, *Pharmacol. Rep.* **2020**, *72*, 1738–1748. https://doi.org/10.1007/s43440-020-00149-4.
[37] S. Kumar, S. Rulhania, S. Jaswal, V. Monga, *Eur. J. Med. Chem.* **2021**, *209*, 112923. https://doi.org/10.1016/j.ejmech.2020.112923.
[38] C. T. Supuran, *Nat. Rev. Drug Discovery* **2008**, *7*, 168–181. https://doi.org/10.1038/nrd2467.
[39] D. Ekinci, Ş. Beydemir, Z. Alim, *Pharmacol. Rep.* **2007**, *59*, 580–587.
[40] K. M. Wilbur, N. G. Anderson, *J. Biol. Chem.* **1948**, *176*, 147–154. https://doi.org/10.1016/S0021-9258(18)51011-5.
[41] M. M. Bradford, *Anal. Biochem.* **1976**, *72*, 248–251. https://doi.org/10.1006/abio.1976.9999.
[42] U. K. Laemmli, *Nature* **1970**, *227*, 680–685. https://doi.org/10.1038/227680a0.
[43] J. A. Verpoorte, S. Mehta, J. T. Edsall, *J. Biol. Chem.* **1967**, *242*, 4221–4229. https://doi.org/10.1016/S0021-9258(18)95800-X.
[44] G. L. Ellman, K. D. Courtney, V. Andres, R. M. Featherstone, *Biochem. Pharmacol.* **1961**, *7*, 88–90. https://doi.org/10.1016/0006-2952(61)90145-9.
[45] A. Angeli, M. Ferraroni, C. T. Supuran, *ACS Med. Chem. Lett.* **2018**, *9*, 1035–1038. https://doi.org/10.1021/acsmedchemlett.8b00334.
[46] J. Cheung, M. J. Rudolph, F. Burshteyn, M. S. Cassidy, E. N. Gary, J. Love, M. C. Franklin, J. J. Height, *J. Med. Chem.* **2012**, *55*, 10282–10286. https://doi.org/10.1021/jm300871x.
[47] P. Mader, J. Brynda, R. Gitto, S. Agnello, P. Pachl, C. T. Supuran, A. Chimirri, P. Rezacova, *J. Med. Chem.* **2011**, *54*, 2522–2526. https://doi.org/10.1021/jm2000213.
[48] R. Thomsen, M. H. Christensen, *J. Med. Chem.* **2006**, *49*, 3315–3321. https://doi.org/10.1021/jm051197e.
[49] H. Bekker, H. Berendsen, E. Dijkstra, S. Achterop, R. Drunen, D. Van Der Spoel, A. Sijbers, H. Keegstra, B. Reitsma, M. Renardus, R. L. DeGroot, J. Nadrchal, H. Bekker, H. J. C. Berendsen, R. van Drunen, R. de Groot, E. J. Dijkstra, M. K. R. Renardus, E. Dijkstra, M. Renardus, R. Vondrumen, D. Vanderspoel, H. J. C. Berendsen, R. V. Drunen, D. V. D. Spoel, H. J. C. Berendsen, E. J. Dijkstra, D. van der Spoel, H. J. Berendsen, D. der Spoel, H. J. C. Berendsen, D. Spoel, A. Sijbers, J. Reitsma, D. R. van der Westhuyzen, *Phys. Comput.* **1993**, *92*, 252–256.
[50] A. Ganesan, M. L. Coote, K. Barakat, *Drug Discovery Today* **2017**, *22*, 249–269. https://doi.org/10.1016/j.drudis.2016.11.001.
[51] R. Rawat, S. M. Verma, *J. Biomol. Struct. Dyn.* **2020**, *38*, 5362–5373. https://doi.org/10.1080/07391102.2019.1700165.
[52] N. Schmid, A. P. Eichenberger, A. Choutko, S. Riniker, M. Winger, A. E. Mark, W. F. Van Gunsteren, *Eur. Biophys. J.* **2011**, *40*, 843–856. https://doi.org/10.1007/s00249-011-0700-9.
[53] D. M. Van Aalten, R. Bywater, J. B. Findlay, M. Hendlich, R. W. Hooft, G. Vriend, *J. Comput.-Aided Mol. Des.* **1996**, *10*, 255–262. https://doi.org/10.1007/BF00355047.
[54] P. Mark, L. Nilsson, *J. Phys. Chem. A* **2001**, *105*, 9954–9960. https://doi.org/10.1021/jp003020w.
[55] W. F. Van Gunsteren, H. J. C. Berendsen, *Mol. Simul.* **1987**, *1*, 173–185. https://doi.org/10.1080/08927028808080941.
[56] H. J. C. Berendsen, D. Van Der Spoel, R. Van Drunen, *Comput. Phys. Commun.* **1995**, *14*, 43–56. https://doi.org/10.1016/0010-4655(95)00042-E.
[57] B. Hess, H. Bekker, H. J. C. Berendsen, J. G. E. M. Fraaije, *J. Comput. Chem.* **1997**, *18*, 1463–1472. https://doi.org/10.1002/(SICI)1096-987X(199709)18:12<1463::AID-JCC4>3.0.CO;2-H.
[58] M. Di Pierro, R. Elber, B. A. Leimkuhler, *J. Chem. Theory Comput.* **2015**, *11*, 5624–5637. https://doi.org/10.1021/acs.jctc.5b00648.
[59] W. Humphrey, A. Dalke, K. Schulten, *J. Mol. Graphics* **1996**, *14*, 33–38. https://doi.org/10.1016/0263-7855(96)00018-5.
[60] R. Rawat, K. Kant, A. Kumar, K. Bhati, S. M. Verma, *Future Med. Chem.* **2021**, *13*, 447–456. https://doi.org/10.4155/fmc-2020-0191.
[61] R. Rawat, S. M. Verma, *J. Biomol. Struct. Dyn.* **2021**, *39*, 5148–5159. 10.1080/07391102.2020.1784288.
[62] A. Vaught, *Linux J.* **1996**, *28*, 7.

Manuscript received: May 14, 2024
Accepted manuscript online: August 25, 2024
Version of record online: October 22, 2024